





Future warming stimulates growth and photosynthesis in an Arctic microalga more strongly than changes in light intensity or pCO₂

Sebastian D. Rokitta ^{1,*} Christian H. Grossmann,¹ Elisa Werner,¹ Jannika Moye,¹ Giulia Castellani ²,
Eva-Maria Nöthig ² Björn Rost ^{1,3}

¹Marine Biogeosciences Division, Alfred-Wegener-Institute – Helmholtz-Centre for Polar and Marine Research, Bremerhaven, Deutschland

²Polar Biological Oceanography Division, Alfred-Wegener-Institute – Helmholtz-Centre for Polar and Marine Research, Am Handelshafen 12, Bremerhaven, 27570, Bremen, Deutschland

³Faculty of Biology/Chemistry, Universität Bremen, Bremen, Germany

Abstract

We assessed the responses of solitary cells of Arctic *Phaeocystis pouchetii* grown under a matrix of temperature (2°C vs. 6°C), light intensity (55 vs. 160 μmol photons m⁻² s⁻¹) and pCO₂ (400 vs. 1000 μatm CO₂, i.e., 40.5 vs. 101.3 Pa). Next to acclimation parameters (growth rates, particulate and dissolved organic C and N, Chlorophyll *a* content), we measured physiological processes in vivo (electron transport rates and net photosynthesis) using fast-repetition rate fluorometry and membrane-inlet mass spectrometry. Within the applied driver ranges, elevated temperature had the most pronounced impacts, significantly increasing growth, elemental quotas and photosynthetic performance. Light stimulations manifested more prominently under 6°C, underlining temperature's role as a “master-variable”. pCO₂ was the least effective driver, exerting mostly insignificant effects. The obtained data were used for a simplistic upscaling simulation to investigate potential changes in *P. pouchetii*'s bloom dynamics in the Fram Strait with increasing temperatures over the 21st century. Although solitary cells might not be fully representative of colonial cells commonly observed in the field, our results suggest that global warming accelerates bloom dynamics, with earlier onsets of blooms and higher peak biomasses. Such a temperature-induced acceleration in the phenology of *Phaeocystis* and likely other Arctic phytoplankton might cause temporal mismatches, e.g., with the development of grazers, and therefore substantially affect the biogeochemistry and ecology of the Arctic.

The haptophyte *P. pouchetii* is a prominent member of Arctic phytoplankton assemblages (Gradinger and Baumann 1991; Degerlund and Eilertsen 2010; Nöthig et al. 2015). *Phaeocystis* is known to often dominate extensive phytoplankton bloom events in the open water close to the marginal ice zone (Assmy et al. 2017), but also increasingly under ice

(Ardyna et al. 2020a; Lannuzel et al. 2020). As part of its life-cycling, flagellated solitary cells can transition into gelatinous colonies, e.g., under high-light conditions (Peperzak 1993), which makes them less prone to predation and apparently stabilizes predator–prey dynamics (Verity et al. 2007; Smith and Trimborn 2023). The species of the *Phaeocystis* genus have also gained much attention due to the extensive production of dissolved organic matter during blooms (Eberlein et al. 1985) that appears to foster the formation of mucous transparent extracellular polysaccharides (TEP; Passow and Wassmann 1994; Schoemann et al. 2005). The co-occurrence of TEP and marine snow during *Phaeocystis*-dominated blooms has led to the conclusion that the mucus promotes aggregation of organic matter and thereby increases particles' sinking rates, i.e., the vertical carbon export (DiTullio et al. 2000; Riebesell et al. 1995). Mineral compounds, such as biogenic calcite and silica from phytoplankton shells, but also cryogenic gypsum crystals can be embedded in *Phaeocystis* aggregates and serve as ballast, furthermore enhancing depth export (Leventer 2003; Wollenburg et al. 2018). Thus, *Phaeocystis* can be an important contributor

*Correspondence: Sebastian.Rokitta@awi.de

This is an open access article under the terms of the [Creative Commons Attribution](https://creativecommons.org/licenses/by/4.0/) License, which permits use, distribution and reproduction in any medium, provided the original work is properly cited.

Additional Supporting Information may be found in the online version of this article.

Author Contribution Statement: S.D.R. and B.R. devised the experiment. C.H.G., E.W., and J.M. did main lab work under supervision of S.D.R. S.D.R., C.H.G., E.W., and J.M. did data evaluation and statistical testing. G.C. and S.D.R. conducted simulations. E.-M.N. contributed expertise on *Phaeocystis* ecology and gave helpful comments throughout the process. The manuscript was drafted by S.D.R., G.C., B.R., and E.-M.N. All authors have approved the submission.

to, and regulator of, vertical carbon fluxes in the subpolar north Atlantic and even ice-covered polar waters.

Within the past years, *P. pouchetii* increasingly dominated phytoplankton blooms in the Arctic (Assmy et al. 2017; Ardyna et al. 2020a; Lannuzel et al. 2020), especially after the years when a warm water anomaly passed through Fram Strait (Soltwedel et al. 2015). This suggests that this species directly benefits from the warming of the Arctic in terms of biomass production and ultimately abundance. Warming induces secondary environmental changes, e.g., enhanced thermal stratification of the upper ocean with less deep-mixing, and therefore, phytoplankton cells receive higher mean insolation in the sunlit mixed layer. The continuous retreat and thinning of sea ice furthermore increase the light availability in the water column and likely also extend the Arctic growing season (AMAP 2018; Ardyna and Arrigo 2020; Arrigo et al. 2008; Steinacher et al. 2010) as well as marginal ice zone area (Nöthig et al. 2020). Lastly, the Arctic ocean is acidifying stronger and more rapidly than other ocean regions, because low temperatures favor the dissolution of CO₂, and due to the input of riverine and glacial meltwater, the lowered alkalinity makes the water more prone to corresponding pH shifts (AMAP 2018; Zhang et al. 2020).

All of these environmental changes have the potential to alter growth and biomass production of phytoplankton. Ocean warming, acidification and changes in irradiance have been shown to interact in many phytoplankton species (Seifert et al. 2020 and references therein), meaning that they can buffer or amplify each other and thus need to be assessed using full-factorial manipulations. Despite *Phaeocystis*' important roles in ecology and biogeochemistry, only few data exist regarding its growth performance under (co-)varying environmental variables, and in vivo physiological data are particularly scarce (e.g., Pfaff et al. 2016). More data are needed since the importance of *Phaeocystis* is increasingly acknowledged in modeling efforts that project the impacts of global change for ecosystem functioning and biogeochemical cycling (Le Quére et al. 2005; Vernet et al. 2017; Smith and Trimborn 2023).

To narrow this knowledge gap, we have grown solitary cells of *P. pouchetii* in dilute-batch cultures and acclimated them to a full-factorial matrix of different temperature, light, and pCO₂ levels. Thereby, we covered constellations between contemporary settings (2°C, 55 μmol photons m⁻² s⁻¹, 400 μatm CO₂ [40.5 Pa]), the environmental settings anticipated under high-emission scenarios for the end of the century (6°C, 160 μmol photons m⁻² s⁻¹, 1000 μatm CO₂ [101.3 Pa]) as well as all individual combinations. We have assessed growth rates, quotas of particulate organic carbon and nitrogen (POC, PON), as well as chlorophyll *a* (Chl *a*) contents and exudation rates of dissolved organic carbon and nitrogen (DOC, DON). In vivo photosynthetic parameters were measured by means of fast-repetition rate fluorometry (FRRf) and membrane-inlet mass spectrometry (MIMS). We have used the acquired physiological data to simplistically simulate and

visualize *Phaeocystis*' growth dynamics for the temperatures projected for the Fram Strait over the coming century.

Material and methods

Culture and experimental conditions

Cultures of Arctic *P. pouchetii* (strain PS78; isolated from the Fram Strait) were grown in sterile-filtered (2 μm, Sartobran 300 capsule filter, Sartorius) Arctic seawater (salinity 33) that was enriched with vitamins and trace metals according to the F/2 recipe (Guillard and Ryther 1962). Additionally, nitrate and phosphate were added in concentrations of 100 and 6 μmol L⁻¹, respectively. As *P. pouchetii* can exist as single cells or in a colonial stage, where multiple single cells embed themselves in a rigid hull (Hamm 2000), we took great care to work only with single cell cultures. Cultures containing colonies have a patchy distribution of biomass, which not only compromises the quantification of cells and biomass, but also hampers proper physiological measurements. To ensure absence of colonies, we used a strain that typically remains in its single-celled stage, which was verified by daily visual inspections, including light microscopy.

To achieve the temperature treatments, cells were cultured either in 2 L-bottles on a roller table in a temperature-stabilized culture room (2 ± 0.5°C) or in 1 L bottles in an incubation cabinet (6 ± 0.5°C; Rumed, Rubart Apparatebau). To avoid differential effects due to bottle curvature and light dispersion, the light intensities (24 : 0 h light : dark cycle) were adjusted to 55 ± 10 and 160 ± 15 μmol photons m⁻² s⁻¹ in situ, using a universal light meter (ULM-500, Walz) equipped with a 4π-quantum sensor (US-SQS/L, Walz) that was immersed in the sea-water filled bottles. These light intensities are typically encountered in the mixed layer and further resemble light limitation and saturation, respectively, without inducing light stress or photoinhibition. To adjust pCO₂ levels, media were aerated (~ 100 mL min⁻¹) with humidified air of 400 or 1000 μatm pCO₂ for at least 12 h prior to inoculation. Gas mixtures were prepared with a custom-made gas mixing system consisting of a mass flow controller (CGM 2000, MCZ Umwelttechnik) that mixes CO₂-free air (Domnick Hunter) with pure CO₂ (Air Liquide). To avoid sedimentation of cells, bottles on the roller table were continuously rotated (~ 15 rpm) while bottles in the incubation cabinet were gently aerated (~ 100 mL min⁻¹) with pCO₂-adjusted gas mixtures.

To monitor carbonate chemistry during the experiment, pH and dissolved inorganic carbon (DIC) were measured alongside with temperature at the onset (*t*₀) and end (*t*_{fin}) of the experiments. The pH and temperature were measured with a mobile pH-meter (826 pH, equipped with an Aquatode Plus; Metrohm) that was 3-point calibrated using buffers certified by the U.S. National Bureau of Standards (NBS). [DIC] was measured colorimetrically with a TRAACS CS800 auto-analyzer (Seal Analytical) according to the method of Stoll et al. (2001). Salinity was determined with a

WTW Multi 340i salinometer (WTW). Calculations on carbonate chemistry were based on [DIC], pH, and temperature, assuming phosphate concentrations of $6 \mu\text{mol L}^{-1}$. Dissociation constants of sulfuric acid (Dickson 1990) and carbonic acid (Mehrbach et al. 1973; Dickson and Millero 1987) were applied. Initial and final carbonate systems of the cultivations are given in Supporting Information S1. Please note that the drift of DIC concentration was $< 5\%$, ensuring stability of pCO_2 treatments.

Acclimation responses

Specific growth rates were calculated from daily increments of exponentially growing single cells using a Multisizer III particle counter (Beckman Coulter). For the determination of particulate organic carbon and nitrogen quotas (POC, PON), cells were harvested onto pre-combusted (500°C , 10 h) glass fiber filters (GF/F, Whatman) and dried overnight at 60°C . Filters were then packed into tin foil and analyzed using a EuroVector EA 3000 CHNS-O elemental analyzer (HEKAtech). For analysis of the Chl *a* content, cells were filtered onto cellulose-nitrate filters ($0.45 \mu\text{m}$ pore size, Sartorius), immediately shock-frozen in liquid nitrogen and stored at -20°C for up to 3 weeks. Samples were extracted by vigorous vortexing in 8 mL of 90% (v/v) acetone and measured on a TD-700 fluorometer (Turner Designs) following the “acidification method” described in the JGOFS protocols (Knap et al. 1996). To estimate potential exudation of dissolved compounds, samples for analyses of dissolved organic carbon and nitrogen (DOC, DON) were taken at t_0 and t_{fin} using glass-fiber syringe-filters (GF/F, $0.7 \mu\text{m}$ pore size; Whatman). Syringes and sample containers were washed twice with ultrapure hydrochloric acid before use to avoid contamination derived from plasticware. Samples were directly frozen and stored at -80°C , and measured after 1–3 weeks in a Total Organic Carbon Analyzer (TOC-L, Shimadzu).

Photosynthesis vs. irradiance response curves

To assess photosynthesis vs. irradiance (P-I) curves of relative Photosystem II electron transfer rates, we made use of fast repetition rate fluorometry (FRRf; FastOcean PTX with FastAct Laboratory system; Chelsea Technologies) as described in Hoppe et al. (2018a). Briefly, the excitation wavelength was set to 450 nm, applying light intensities of up to 20 mmol photons $\text{m}^{-2} \text{s}^{-1}$. The FRRf was used in single turnover mode, with a saturation phase comprising 100 flashlets of $2 \mu\text{s}$ pitch and a relaxation phase comprising 40 flashlets on a $50 \mu\text{s}$ pitch. All measurements were conducted in a temperature-stabilized cuvette at the respective incubation temperature (stability $\pm 1^\circ\text{C}$). The minimum (F_0) and maximum chlorophyll fluorescence (F_m) were derived from iterative fitting of the induction phase (Kolber et al. 1998) and the relaxation phase (Oxborough et al. 2012).

To assess P-I curves of net photosynthesis, membrane-inlet mass spectrometry MIMS was applied as described in

Kottmeier et al. (2016). The setup of the MIMS consisted of a light-adjustable and temperature-controlled 8 mL cuvette coupled to a sector-field multicollector mass spectrometer (Isoprime, GV Instruments) via a gas-permeable 0.01 mm polytetrafluorethylene-membrane (Reichert Chemietechnik). After passing the membrane, O_2 is conducted into the mass spectrometer via an evacuated tubing system, so that the photosynthetic and respiratory activities can be monitored during light and dark intervals, respectively. Algae were concentrated by gentle filtration using polycarbonate filters ($4 \mu\text{m}$ pore-size; Merck Millipore) and washed three times with 10 mL 50 mM HEPES-buffered, DIC-free F/2 medium to exchange the culturing-media. Afterwards, the concentrated, but translucent cell culture (Chl *a* concentrations $< 0.5 \mu\text{g mL}^{-1}$) was transferred to the cuvette. During the transfer into the assay buffer, cells were kept at the incubation temperature $\pm 1^\circ\text{C}$. NaHCO_3^- solution was subsequently added to final concentrations of $\sim 2.1 \text{ mmol L}^{-1}$ to establish normal DIC backgrounds. After a pre-acclimation step (3–6 min of light followed by 6 min of darkness), P-I curves were assessed in consecutive 6 min light : dark intervals with increasing light intensities. Net photosynthesis was determined by calculating the steady-state O_2 fluxes during the late light phase and was normalized to Chl *a* concentrations in the cuvette.

Least-squares regression was used on both, FRRf and MIMS data, to derive the maximum rates of electron transfer ($V_{\text{max}; \text{ETR}}$) and net photosynthesis ($V_{\text{max}; \text{PS}}$) as well as the associated light acclimation indices ($I_{k; \text{ETR}}$, $I_{k; \text{PS}}$) and maximum light-use efficiencies (α_{ETR} , α_{PS}) using the photosynthesis function of Rokitta and Rost (2012) (Eqs. 1–3):

$$V = V_{\text{max}} \times \left(1 - e^{-(b \times (I - c))}\right) \quad (1)$$

$$I_k = b^{-1} + c \quad (2)$$

$$\alpha = V_{\text{max}} \times b \quad (3)$$

Statistics

For statistical significance testing, 3-way ANOVAs were used on the data matrix of temperature vs. light vs. pCO_2 . Significant differences between means were obtained by Newman-Keuls post-hoc statistics as implemented in the DescTools package in R (R Core Team 2014). Differences were judged significant when p-values were < 0.05 . Obtained results of statistical testing can be found in the Supporting Information S2. Throughout this study, the number of biological replicates was ≥ 3 , and error bars depict the standard deviation.

Results

Experimental outcomes

Specific growth rates of *P. pouchetii* were most strongly affected by temperature (Fig. 1a): under low temperature (2°C), the growth rates were $\sim 0.38 \text{ d}^{-1}$ throughout all treatments,

i.e., they were unaffected by either light (55 vs. 160 $\mu\text{mol photons m}^{-2} \text{s}^{-1}$) or pCO_2 (400 vs. 1000 $\mu\text{atm CO}_2$). Under high temperature (6°C), however, growth rates were up to 25% higher, and the temperature stimulation was strongest in the high-light/high- pCO_2 treatment, yielding growth rates of $\sim 0.52 \text{ d}^{-1}$.

Also, the quotas of particulate organic carbon and nitrogen (POC and PON; Fig. 1b,c) changed most strongly in response to the temperature increase, whereas light and pCO_2 had no significant effects: While POC quotas in the low temperature treatments ranged from 19 to 21 pg cell^{-1} , warming caused 40–65%

increased POC quotas ranging from 26 to 36 pg cell^{-1} . Likewise, PON quotas were 3.0–3.6 pg cell^{-1} in the low temperature treatment, and warming resulted in PON quotas between 4.9 and 6.0 pg cell^{-1} . Since both quotas responded similarly to the applied treatment, the atomic C : N ratios (Fig. 1d) were not significantly affected by any of the applied treatments and ranged between 6.3 and 7.2 throughout the dataset.

Due to the described trends in growth rates and quotas, also the calculated production rates of POC and PON (Fig. 1e,f) showed the strongest responses to high temperature: Both rates hardly responded to light intensity or pCO_2 under

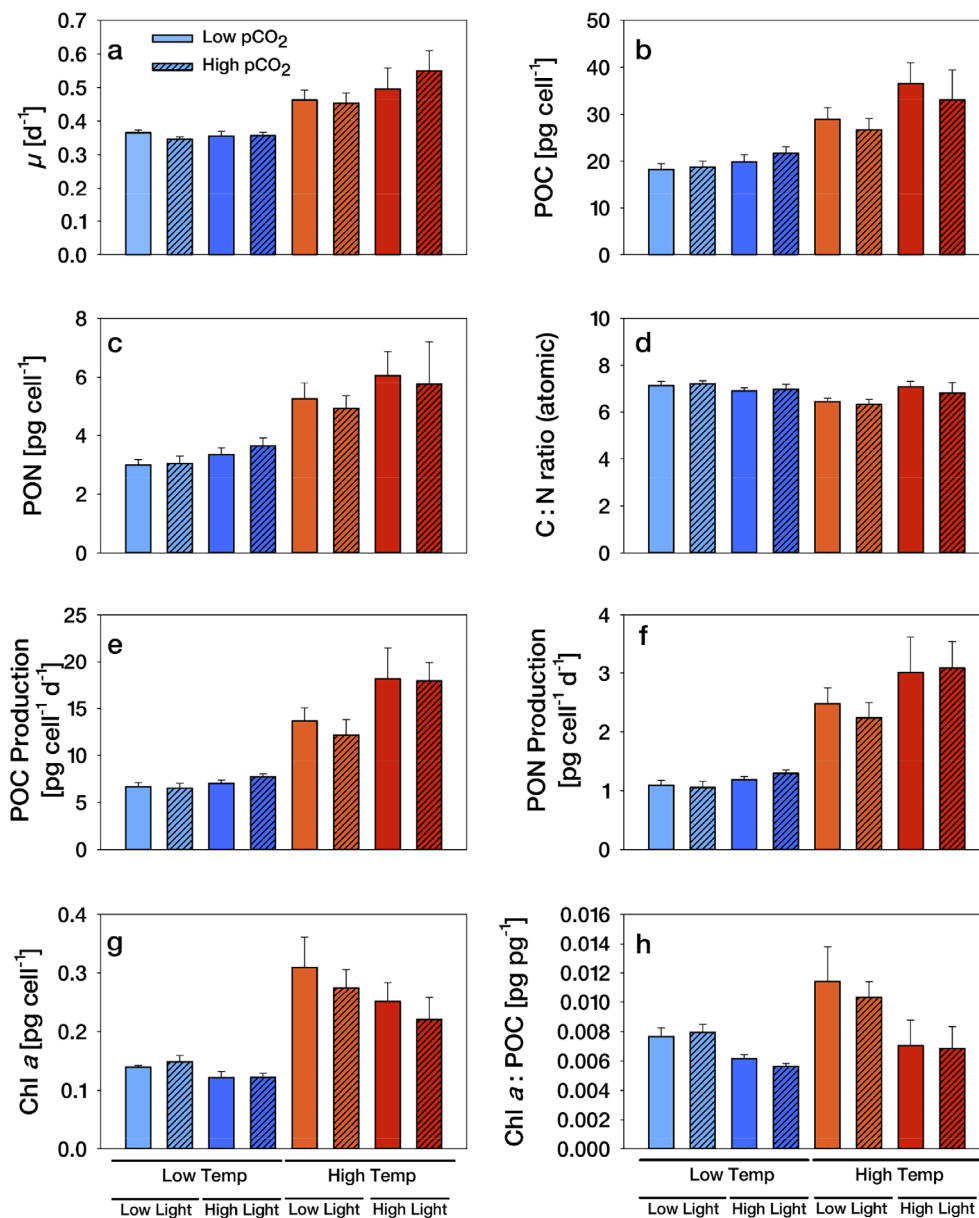


Fig. 1. Responses of *P. pouchetii* in growth rate (a), quotas, ratios, and production rates of POC and PON (b–f) as well as quotas and ratios of Chl *a* (g, h) toward elevated temperature (red colors), light intensity (darker color tone) and pCO_2 (hatched). Significances are reported in Supporting Information Fig. S2.

low temperature, leading to statistically indifferent production rates ranging from 6.5 to 7.7 and 1.0 to 1.3 $\mu\text{g cell}^{-1} \text{d}^{-1}$ for POC and PON, respectively. Under high temperature, however, production rates roughly doubled with 12.1–18.1 and 2.2–3.0 $\mu\text{g cell}^{-1} \text{d}^{-1}$ for POC and PON, respectively.

The cellular Chl *a* quotas (Fig. 1g) ranged from 0.12 to 0.14 $\mu\text{g cell}^{-1}$ in the low temperature treatment and increased strongly by up to 122% in response to warming, with values in some treatments reaching up to 0.31 $\mu\text{g cell}^{-1}$. While the mean Chl *a* quotas were generally lower in the high-light treatments than in the low-light treatments, these effects were not significant. Likewise, high pCO_2 did not have any significant effect on Chl *a* quotas. POC-normalized Chl *a* contents (Fig. 1h) showed similar patterns, i.e., Chl *a* : POC was up to 30% higher in the high temperature treatment compared to the low temperature treatment and was consistently lower under high-light than under low-light intensities. Also here, no significant effects of high pCO_2 could be determined.

Since *Phaeocystis* has been reported to be a prominent producer of DOC and DON, we assessed the exudation of these compounds during the cultivation. In contrast to our expectation, DOC and DON were not released in relevant amounts (Supporting Information S4). Instead, data sometimes even indicated a slight uptake of DOC and DON in the range of few percent compared to its own specific growth rate. Due to large uncertainties, no further quantitative statements could yet be made about the DOC/DON turnover.

Photosynthetic $V_{\text{max};\text{rETR}}$, as derived from FRRf-based P-I curves (Fig. 2a), was substantially increased in response to high temperatures, with stimulations between 170% and 300%. While under low temperature, there were no significant effects of light or pCO_2 , under high temperature, high-light increased $V_{\text{max};\text{rETR}}$ by $\sim 40\%$. In none of the treatments, significant pCO_2 effects on $V_{\text{max};\text{rETR}}$ could be determined. The light acclimation index $I_{k;\text{rETR}}$, as determined by FRRf (Fig. 2b), was on average $\sim 90 \mu\text{mol photons m}^{-2} \text{s}^{-1}$ under low temperature, but strongly increased under high temperature, reaching ~ 145 and $\sim 260 \mu\text{mol photons m}^{-2} \text{s}^{-1}$ in the low- and high-light treatments, respectively. Like in many other parameters, there was no significant effect of pCO_2 on $I_{k;\text{rETR}}$. The light use efficiency α_{rETR} (Fig. 2c) was increased by high temperature, the effect being larger under low-light (+38%) than under high-light (+20%). Conversely, high-light did not affect α_{rETR} under low temperature, but decreased it (–21%) under high temperature. An effect of pCO_2 was only significant in the low temperature treatments, with values being higher under low-light (+13%) and high-light (+26%).

MIMS-based P-I curves were obtained in the cells acclimated to low temperatures, where high-light stimulated $V_{\text{max};\text{net}}$ by 20% under low, but not under high pCO_2 (Fig. 2a, green bars). High pCO_2 itself increased the $V_{\text{max};\text{net}}$ by 38% in low-light, but only by 18% under high-light. The light

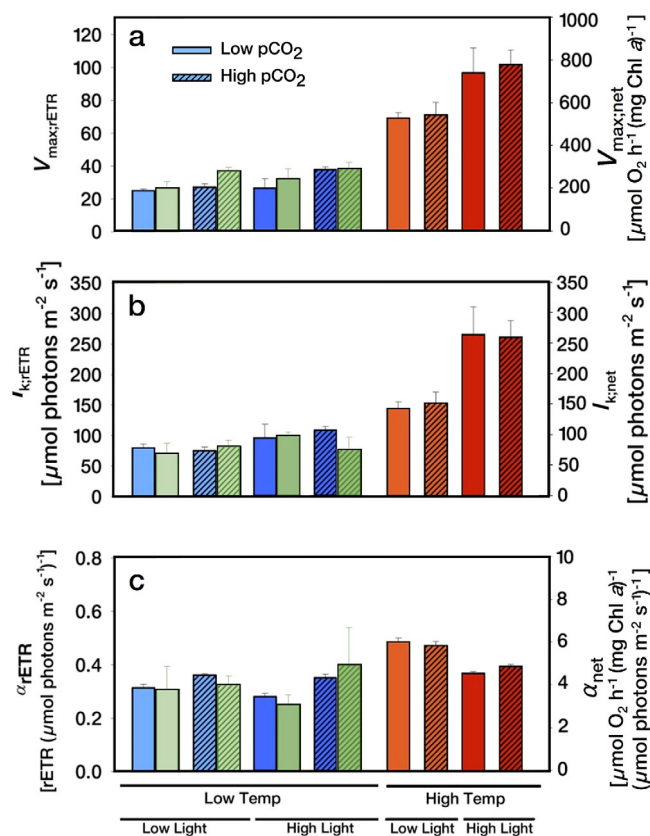


Fig. 2. Responses of *P. pouchetii* in FRRf-derived P-I parameters $V_{\text{max};\text{rETR}}$, $I_{k;\text{rETR}}$, and α_{rETR} (a–c) toward elevated temperature (red colors), light intensity (darker color tone) and pCO_2 (hatched). MIMS-derived P-I parameters $V_{\text{max};\text{net}}$, $I_{k;\text{net}}$, and α_{net} are plotted as green bars juxtaposed to the according treatments. Note that MIMS-based data could not be obtained for the high temperature treatment. Significances are reported in Supporting Information S2.

acclimation index $I_{k;\text{net}}$ (Fig. 2b, green bars) ranged between 70 and 100 $\mu\text{mol photons m}^{-2} \text{s}^{-1}$ in the low temperature treatments. The light use efficiency α_{net} (Fig. 2c, green bars) ranged around 4 $\mu\text{mol O}_2 (\text{mg Chl } a)^{-1} \text{h}^{-1}$ ($\mu\text{mol photons m}^{-2} \text{s}^{-1})^{-1}$ in all low temperature treatments. No significant effects of pCO_2 on I_k and α_{net} could be determined in any of the treatments. P-I curves could not be obtained from cells acclimated to high temperatures, as the concentration procedure apparently harmed these cells: After the required concentration step, high-temperature acclimated cells aggregated and showed no stable photosynthesis and respiration signals, rendering the assessments of P-I curves impossible. Since the concentration procedure worked well for cells acclimated to low temperatures, the high temperature must have affected the cellular integrity or surface properties, making cells highly sensitive to the handling. Multiple attempts were made to concentrate cells more gently, including different protocols of gentle centrifugation, but whenever cells were inserted into the stirred MIMS cuvette, the biomass started to clog (see Discussion).

Discussion

Temperature is the prime driver for ecophysiological responses

Throughout the dataset, temperature was the prime driver of observed responses in *P. pouchetii*, followed by light (Figs. 1, 2). Compared to these drivers and their applied values, the effects of the applied pCO₂ range were small and mostly insignificant. Obviously, the responses toward individual drivers and their combinations change with treatment doses, but since all the driver levels were chosen to mimic typical present-day vs. high emission scenarios for end-of-the-century, it can be concluded that changes in temperature and light likely have the largest influence on *Phaeocystis*, while pCO₂ and resulting ocean acidification are of minor importance for this species. This is in line with other studies, finding Arctic phytoplankton assemblages (Thoisen et al. 2015; Hoppe et al. 2018b) and single Arctic key species (Wolf et al. 2018; White et al. 2020) to respond positively to warming and/or higher light levels, while they were relatively resilient toward elevated pCO₂ over a wide range of temperatures and light intensities.

In *P. pouchetii*, elevated temperatures led to significant stimulations in growth and production rates, evidenced by the higher POC and PON quotas as well as photosynthesis performance (Figs. 1, 2). Overall, assessed quotas and production rates of POC and PON under low temperature are slightly higher than previously observed in solitary *P. pouchetii* cells from Norwegian waters grown under comparable conditions (Verity et al. 1991), but well in line with data compiled from several studies on (also colonial) *Phaeocystis* as compiled in Peperzak et al. (2015). Likewise, growth rates and cellular C : N ratios obtained in our study agree well with the mentioned studies. Moreover, variations in cell size and thus quotas and cell-specific production rates are common among different strains and regional types of *P. pouchetii* (Verity et al. 1991). Despite stimulations in both POC and PON quotas, the C : N ratios were more or less unaffected by warming. Based on findings from diatoms (Young et al. 2015) one could have expected that the applied warming benefits the efficiency of RubisCO, thereby allowing for lower quantities of this N-rich enzyme and, in turn, higher C : N ratios. The here obtained data, however, suggest that in the haptophyte *P. pouchetii*, C and N metabolism are positively, but not differentially affected by warming.

Environmental drivers modulate each other

The general modulation of light responses by temperature underlines that temperature is a “master-variable” for biological processes (Hancke et al. 2008; Thompson et al. 1992; Toseland et al. 2013) that engages either in an additive, synergistic or antagonistic manner with other environmental drivers (Sett et al. 2014; Seifert et al. 2020). Elevated temperature and light intensity were found to synergistically interact

in our study: Under low temperature, high-light did not significantly affect growth rates, quotas or production rates of POC and PON (Fig. 1a–f), although Chl *a* quotas and Chl *a* : POC ratios (Fig. 1g,h) indicated that photo-acclimation to high-light was indeed happening. This photo-acclimation could, however, not translate into significant changes of, e.g., biomass production. Under high temperature, in contrast, high-light became effective and significantly stimulated growth rates, quotas and production rates of POC and PON (Fig. 1a–f). Apparently, these processes become more efficient with warming and shift the physiological bottleneck more toward the light reactions. This is also reflected by the P-I parameters, i.e., $V_{\max:rETR}$, α_{rETR} and $I_{k:rETR}$ (Fig. 2), which do not experience light effects at low temperatures, but under high temperatures. This temperature stimulation can be attributed to faster molecular processes in the photosynthetic electron transport chains, causing faster re-opening times of photosystem II, and shorter photochemical turnover times (Falkowski 1980), as has been previously observed in Antarctic psychrophilic phytoplankton assemblages (Tilzer et al. 1986). In other words, cells in a warmer environment are better able to utilize high photon fluxes, leading to the observed synergistic interaction between the drivers temperature and light.

The here observed benefit of higher temperature, however, will unlikely manifest uniformly across wide temperature gradients, as also indicated in Peperzak (2003). In that study, *Phaeocystis globosa* was cultivated at temperatures of 18°C and growth ceased rapidly in response to a 4°C temperature elevation. Since physiological rates will reach their maximum at a specific temperature but rapidly decline at higher temperatures due to stress and unbalanced growth, it is likely that the applied ‘low’ temperatures in that study were already close to the species’ thermal optimum. As a consequence, the applied temperature elevation of 4°C likely pushed the cells beyond their optimum and caused cell death. These apparent contrasting results between temperature treatments (i.e., the same temperature differences) highlight the importance of obtaining more species- and habitat-specific temperature performance curves across a wider range of temperatures, because without this species-specific context, depending on the choice of treatment temperatures, it is possible to measure stimulation, inhibition or unaltered rates in response to a temperature treatment.

Within the tested driver space of our study, pCO₂ was the least influential driver. Under the low temperature setting, effects of pCO₂ on growth rates and Chl *a* quotas were negligible, and even when an effect was detected, it was small compared to those caused by high-light (cf. quotas and production rates of POC and PON; Fig. 1b–f). Also under the high temperature setting, where photosynthesis was less throttled and therefore able to scale better with light, increased pCO₂ caused only insignificant or numerically negligible effects. These results contrast the responses observed for the chlorophyte *Micromonas pusilla*, where elevated pCO₂ caused slightly

negative effects on POC production under low, but prominently positive effects under high temperature (Hoppe et al. 2018a). Also in that study, temperature (2°C vs. 6°C) was a more important driver than pCO₂ (400 vs. 1000 μatm). The absence of significant CO₂ effects in our study is in line with the idea of a constitutive CO₂-concentrating mechanism in *Phaeocystis*, and *Phaeocystis*' ability to take up CO₂ as well as HCO₃⁻ in roughly equal proportions (Rost et al. 2006; data not shown).

No exudation of dissolved organic matter was observed

P. pouchetii was often reported to exude dissolved organic carbon and nitrogen (DOC, DON), and is thus thought to contribute substantially to the formation of transparent exopolymeric particles (Passow and Wassmann 1994). Consequently, we hypothesized that environmental factors like temperature, light and CO₂ might affect the exudation of DOC and DON. Throughout our experiments, however, no significant exudation of DOC or DON was observed (Supporting Information S3). On the contrary, some results would even suggest a small uptake of DOC and DON. Under similar light intensities and nutrient supplementation, Verity et al. (1991) observed also only minor fractions of the overall C fixation being channeled into DOC. This fraction was estimated to be ~ 3% for single cells, but up to 64% in colonial *P. pouchetii* (Guillard and Hellebust 1971), which led to the notion that the colonial stage is primarily responsible for the production of DOC/N. Accordingly, also the here obtained data indicate that prominent exudation is not a generic feature of *P. pouchetii* per se, but rather a trait of colonial cells (Hamm 2000). Additionally, DOC/N exudation has been observed in a range of environmental conditions, also excess light, which is in line with the observation that high-light levels favor colony formation in the closely related *P. globosa* (Peperzak 1993; Riegman and Van Boekel 1996). Nutrient limitation might also represent such a situation, when photosynthate cannot be used to create new biomass and thus is exudated. This could explain the occurrence of mucus under nutrient-limiting “late bloom” conditions in the field, but not in nutrient-replete experiments (this study; Verity et al. 1991). Future research should assess whether nutrient-limiting conditions trigger DOC/N production also in the solitary cells of *Phaeocystis*.

Observed responses suggest earlier and more rapid blooms dynamics

In order to visualize the potential consequences of our findings for *Phaeocystis*' growth behavior during this century, we used the measured physiological rates and obtained photosynthetic performance parameters for a simplistic upscaling simulation. This was based on the SIMBA model (Castellani et al. 2017), which was reduced to only the phytoplankton module, and forced with the warming anticipated for the current century (RCP 8.5 emission scenario; Meinshausen

et al. 2011). The photosynthesis parametrization was derived from the photosynthetic O₂ fluxes obtained by MIMS. The detailed mathematical underpinnings of the simulation and a basic evaluation of its functionality as well as temperature- and light-sensitivity is available in supporting information S4. Overall, we have performed 94 simulation runs, one for every year from 2006 to 2100. These runs were constrained with a smoothed annual cycle of local light intensity, but with local daily temperatures smoothed over monthly averages as predicted by IPSL-CM5A-LR CMIP5 models running the RCP 8.5 high-emission scenario.

Under this scenario, *Phaeocystis*' bloom phenology in the Fram Strait shows a tendency to be notably accelerated (Fig. 3): Early in the 21st century, the simulated “in-silico” blooms start around late August, while toward the end of the century, blooms are projected to happen as early as the beginning of July, i.e., about 30–40 d earlier. In reality, *Phaeocystis* abundances typically peak between May and July in the Fram Strait (Assmy et al. 2017; Orkney et al. 2020), i.e., our basic upscaling approach has a general offset and places the blooms late in the year, when only a small seeding population is inserted into the model. A larger initial standing stock biomass could have caused an advancement of bloom peaks to more realistic times, but this was not the focus of the study. More importantly, the combined effects of rising temperature and irradiance on the bloom timing seemed to be well

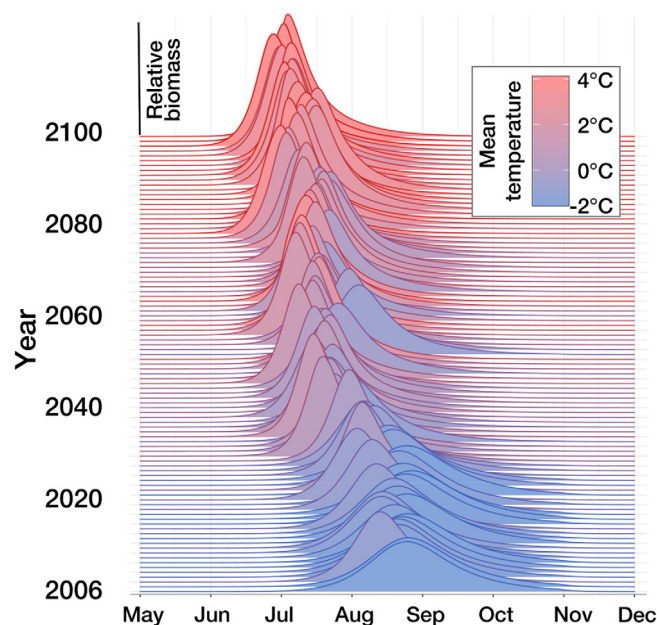


Fig. 3. Simulated bloom phenologies of *P. pouchetii* in the Fram Strait for every year over the 21st century, starting 2006. Bloom dynamics, represented here by the depicted relative biomass, are driven by increasing surface temperatures as projected by IPSL-CM5A-LR CMIP5 model running the RCP 8.5 scenario. Coloration of histograms reflects the mean SST over the growing season (March–October). The height of the curve represents biomass.

resolved: According to our simulations, the anticipated warming will advance the bloom onsets by 4 to 5 d every decade. This is well in line with the observed acceleration in phytoplankton spring phenology of up to 7.5 d per decade (Hoegh-Guldberg et al. 2014; Chivers et al. 2020) and projections of up to 40 d by the end of the century (Cooley et al. 2022). Interestingly, despite using the same light intensity in every simulation, there is not always a perfect correlation with the timing of the bloom peak and the average temperature over the growing season (cf. coloration of Fig. 3). This is because the simulations are constrained with smoothed temperatures, which provide daily values and not a step function for every month. Consequently, the single runs can have similar bloom onsets, e.g., when the temperatures are similar at the beginning of spring, but then also have different peak times when one year has a warmer summer than another one.

It must be emphasized, however, that these simulations are no projections for the future Fram Strait ecosystem. They are simple visualizations of the altered growth behavior under higher temperatures as we measured it in our experiments and physiological assays (Figs. 1, 2). The here used projections of the sea surface-temperatures themselves (IPSL-CM5A-LR CMIP5 outputs) also bear significant uncertainties, especially the further they extend into the future. Lastly, these simplistic simulations intentionally disregard ecological interactions: Competition with other phytoplankton, for example, is not depicted, despite observations that, e.g., diatoms can outcompete *Phaeocystis*, presumably when high-silicate nutrient regimes prevail (Ardyna et al. 2020b). Likewise, effects of different grazers and their potential responses to warming have been neglected, even though such components can have strong influence on bloom dynamics (Karakuş et al. 2021).

Despite these limitations, our data and simulations show that warming will likely accelerate *Phaeocystis*' growth and bloom phenology. Under the assumption that most other phytoplankton will respond similarly to increased temperatures, i.e., with intensified photosynthesis and higher growth rates (e.g., Toseland et al. 2013), the larger-scale implication of our study is that new production (Eppley and Peterson 1979), in particular bloom events, tend to generally occur earlier in the season. In our simulations, the synergistic interaction between increased temperature and light was regarded on a photophysiological basis only. However, effects on the ecosystem level are likely to be amplified in those regions where ice-cover is rapidly ceasing and the light-regime is changing more drastically (Nicolaus et al. 2012). Consequently, food availability for first-order consumers, e.g., copepods or fish larvae may be restricted to earlier times in the year. As temperature-driven shifts in seasonal activities of these consumers tend to be less strong (Cooley et al. 2022), there is an increasing risk of temporal mismatches between primary production and the ontogenetic development of the consumers (Søreide et al. 2010; Dezutter et al. 2019; Randelhoff et al. 2020; Constable et al. 2022). Such differential temperature responses

might thus have far-reaching implications for Arctic food webs, and ultimately also the functioning of the biological carbon pump.

In conclusion, we advocate that the important genus *Phaeocystis* should be included as a canonical phytoplankton functional type in future ecosystem models. Such models should also aim to account for interactive effects, as observed here for light and temperature. Regardless of *Phaeocystis*' mathematical implementation, syn-ecological aspects, like competition among phytoplankton, or grazer responses to global change, should be implemented in more sophisticated ecosystem models.

Data availability statement

The obtained raw replicate data have been archived in the PANGAEA repository under <https://doi.pangaea.de/10.1594/PANGAEA.948489> (Rokitta et al. 2022).

References

- AMAP. 2018. Arctic monitoring and assessment programme (AMAP). Arctic Ocean Acidification. 187pp.
- Ardyna, M., and K. R. Arrigo. 2020. Phytoplankton dynamics in a changing Arctic Ocean. *Nat. Clim. Change* **10**: 892–903.
- Ardyna, M., and others. 2020a. Under-ice phytoplankton blooms: Shedding light on the “invisible” part of Arctic primary production. *Front. Mar. Sci.* **7**: 1–25.
- Ardyna, M., and others. 2020b. Environmental drivers of under-ice phytoplankton bloom dynamics in the Arctic Ocean. *Elementa Sci. Anthropocene* **8**: 1–21.
- Arrigo, K. R., G. van Dijken, and S. Pabi. 2008. Impact of a shrinking Arctic ice cover on marine primary production. *Geophys. Res. Lett.* **35**: 1–6.
- Assmy, P., and others. 2017. Leads in Arctic pack ice enable early phytoplankton blooms below snow-covered sea ice. *Sci. Rep.* **7**: 40850.
- Castellani, G., M. Losch, B. A. Lange, and H. Flores. 2017. Modeling Arctic Sea-ice algae: Physical drivers of spatial distribution and algae phenology. *J. Geophys. Res. Oceans* **122**: 7466–7487.
- Chivers, W. J., M. Edwards, and G. C. Hays. 2020. Phenological shuffling of major marine phytoplankton groups over the last six decades. *Divers. Distrib.* **26**: 536–548.
- Constable, A. J., and others. 2022. Cross-chapter paper 6: Polar regions. *In* H. O. Pörtner and others [eds.], *Climate change 2022: Impacts, adaptation, and vulnerability. Contribution of Working Group II to the Sixth Assessment Report of the Intergovernmental Panel on Climate Change*. Cambridge University Press.
- Cooley, S. R., and others. 2022. Ocean and coastal ecosystems and their services. *Climate change 2022: Impacts, adaptation, and vulnerability. In* Contribution of working group II to the sixth assessment report of the intergovernmental

- panel on climate change. Contribution of working group II to the sixth assessment report of the intergovernmental panel on climate change. Cambridge University Press.
- Degerlund, M., and H. C. Eilertsen. 2010. Main species characteristics of phytoplankton spring blooms in NE Atlantic and Arctic waters (68–80° N). *Estuaries Coast.* **33**: 242–269.
- Dezutter, T., C. Lalande, C. Dufresne, G. Darnis, and L. Fortier. 2019. Mismatch between microalgae and herbivorous copepods due to the record sea ice minimum extent of 2012 and the late sea ice break-up of 2013 in the Beaufort Sea. *Prog. Oceanogr.* **173**: 66–77.
- Dickson, A. G. 1990. Standard potential of the reaction: $\text{AgCl(s)} + \frac{1}{2} \text{H}_2(\text{g}) = \text{Ag(s)} + \text{HCl(aq)}$, and the standard acidity constant of the ion HSO_4^- in synthetic seawater from 273.15 to 318.15 K. *J. Chem. Thermodyn.* **22**: 113–127.
- Dickson, A. G., and F. J. Millero. 1987. A comparison of the equilibrium-constants for the dissociation of carbonic-acid in seawater media. *Deep Sea Res.* **34**: 1733–1743.
- DiTullio, G. R., and others. 2000. Rapid and early export of *Phaeocystis antarctica* blooms in the Ross Sea, Antarctica. *Nature* **404**: 595–598.
- Eberlein, K., M. T. Leal, K. D. Hammer, and W. Hickel. 1985. Dissolved organic substances during a *Phaeocystis pouchetii* bloom in the German bight (North Sea). *Mar. Biol.* **89**: 311–316.
- Eppley, R. W., and B. J. Peterson. 1979. Particulate organic matter flux and planktonic new production in the deep ocean. *Nature* **282**: 677–680.
- Falkowski, P. 1980. Light-shade adaptation in marine phytoplankton, p. 99–119. *In* P. Falkowski [ed.], *Primary productivity in the sea*. Plenum Press.
- Gradinger, R. R., and M. E. M. Baumann. 1991. Distribution of phytoplankton communities in relation to the large-scale hydrographical regime in the Fram Strait. *Mar. Biol.* **111**: 311–321.
- Guillard, R. R. L., and J. A. Hellebust. 1971. Growth and the production of extracellular substances by two strains of *Phaeocystis pouchetii*. *J. Phycol.* **7**: 330–338.
- Guillard, R. R. L., and J. H. Ryther. 1962. Studies of marine planktonic diatoms. *Can. J. Microbiol.* **8**: 229–239.
- Hamm, C. E. 2000. Architecture, ecology and biogeochemistry of *Phaeocystis* colonies. *J. Sea Res.* **43**: 307–315.
- Hancke, K., T. B. Hancke, L. M. Olsen, G. Johnsen, and R. N. Glud. 2008. Temperature effects on microalgal photosynthesis-light responses measured by O_2 production, pulse-amplitude-modulated fluorescence, and ^{14}C assimilation. *J. Phycol.* **44**: 501–514.
- Hoegh-Guldberg, O., and others. 2014. The ocean, p. 1655–1731. *In* IPCC [ed.], *Climate change 2014: Impacts, adaptation, and vulnerability, part B: Regional aspects*. Cambridge University Press.
- Hoppe, C. J. M., C. M. Flintrop, and B. Rost. 2018a. The Arctic picoeukaryote *Micromonas pusilla* benefits synergistically from warming and ocean acidification. *Biogeosciences* **15**: 4353–4365.
- Hoppe, C. J. M., and others. 2018b. Resistance of Arctic phytoplankton to ocean acidification and enhanced irradiance. *Polar Biol.* **41**: 399–413.
- Karakuş, O., and others. 2021. Modeling the impact of macrozooplankton on carbon export production in the Southern Ocean. *J. Geophys. Res. Oceans* **126**: e2021JC017315.
- Knap, A., A. Michaels, A. Close, H. Ducklow, and A. Dickson. 1996. Protocols for the joint global ocean flux study (JGOFS) core measurements. UNESCO.
- Kolber, Z. S., O. Prášil, and P. G. Falkowski. 1998. Measurements of variable chlorophyll fluorescence using fast repetition rate techniques: Defining methodology and experimental protocols. *Biochim. Biophys. Acta* **1367**: 88–106.
- Kottmeier, D. M., S. D. Rokitta, and B. Rost. 2016. Acidification, not carbonation, is the major regulator of carbon fluxes in the coccolithophore *Emiliania huxleyi*. *New Phytol.* **211**: 126–137.
- Lannuzel, D., and others. 2020. The future of Arctic Sea-ice biogeochemistry and ice-associated ecosystems. *Nat. Clim. Change* **10**: 983–992.
- Le Quééré, C., and others. 2005. Ecosystem dynamics based on plankton functional types for global ocean biogeochemistry models. *Glob. Chang. Biol.* **11**: 2016–2040.
- Leventer, A. 2003. Particulate flux from sea ice in polar waters, p. 303–332. *In* *Sea ice: An introduction to its physics, chemistry, biology and geology*. Blackwell Science.
- Mehrbach, C., C. H. Culberson, J. E. Hawley, and R. M. Pytkowicz. 1973. Measurement of the apparent dissociation constants of carbonic acid in seawater at atmospheric pressure. *Limnol. Oceanogr.* **18**: 897–907.
- Meinshausen, M., and others. 2011. The RCP greenhouse gas concentrations and their extensions from 1765 to 2300. *Clim. Change* **109**: 213–241.
- Nicolaus, M., C. Katlein, J. Maslanik, and S. Hendricks. 2012. Changes in Arctic Sea ice result in increasing light transmittance and absorption. *Geophys. Res. Lett.* **39**: 1–6.
- Nöthig, E.-M., and others. 2015. Summertime plankton ecology in Fram Strait—A compilation of long- and short-term observations. *Polar Res.* **34**: 23349.
- Nöthig, E.-M., and others. 2020. Summertime chlorophyll *a* and particulate organic carbon standing stocks in surface waters of the Fram Strait and the Arctic Ocean (1991–2015). *Front. Mar. Sci.* **7**: 1–15.
- Orkney, A., T. Platt, B. E. Narayanaswamy, I. Kostakis, and H. A. Bouman. 2020. Bio-optical evidence for increasing *Phaeocystis* dominance in the Barents Sea. *Philos. Trans. A Math. Phys. Eng. Sci.* **378**: 20190357.
- Oxborough, K., C. M. Moore, D. J. Suggett, T. Lawson, H. G. Chan, and R. J. Geider. 2012. Direct estimation of functional PSII reaction center concentration and PSII electron flux on a volume basis: A new approach to the analysis of

- fast repetition rate fluorometry (FRRf) data. *Limnol. Oceanogr. Methods* **10**: 142–154.
- Passow, U., and P. Wassmann. 1994. On the trophic fate of *Phaeocystis pouchetii* (Hariot): IV. The formation of marine snow by *P. pouchetii*. *Mar. Ecol. Prog. Ser.* **104**: 153–161.
- Peperzak, L. 1993. Daily irradiance governs growth rate and colony formation of *Phaeocystis* (Prymnesiophyceae). *J. Plankton Res.* **15**: 809–821.
- Peperzak, L. 2003. Climate change and harmful algal blooms in the North Sea. *Acta Oecol.* **24**: S139–S144.
- Peperzak, L., H. J. van der Woerd, and K. R. Timmermans. 2015. Disparities between in situ and optically derived carbon biomass and growth rates of the prymnesiophyte *Phaeocystis globosa*. *Biogeosciences* **12**: 1659–1670.
- Pfaff, S., and others. 2016. Ecophysiological plasticity in the Arctic phytoplankton species *Phaeocystis pouchetii* (Prymnesiophyceae, Haptophyta). *Algal Stud.* **151**: 87–102.
- R Core Team. 2014. R: A language and environment for statistical computing. R Foundation for Statistical Computing.
- Randelhoff, A., and others. 2020. Pan-Arctic Ocean primary production constrained by turbulent nitrate fluxes. *Front. Mar. Sci.* **7**: 1–15.
- Riebesell, U., M. Reigstad, P. Wassmann, T. Noji, and U. Passow. 1995. On the trophic fate of *Phaeocystis pouchetii* (Hariot): VI. Significance of *Phaeocystis*-derived mucus for vertical flux. *Neth. J. Sea Res.* **33**: 193–203.
- Riegman, R., and W. Van Boekel. 1996. The ecophysiology of *Phaeocystis globosa*: A review. *J. Sea Res.* **35**: 235–242.
- Rokitta, S. D., and B. Rost. 2012. Effects of CO₂ and their modulation by light in the life-cycle stages of the coccolithophore *Emiliania huxleyi*. *Limnol. Oceanogr.* **57**: 607–618.
- Rokitta, S. D., and others. 2022. *Phaeocystis pouchetii*'s responses to temperature (2 vs. 6 °C), light (55 vs. 160 μmol photons m⁻² s⁻¹) and pCO₂ (400 vs. 1000 μatm). PANGAEA; doi.pangaea.de/10.1594/PANGAEA.948489
- Rost, B., U. Riebesell, and D. Sültemeyer. 2006. Carbon acquisition of marine phytoplankton: Effect of photoperiod length. *Limnol. Oceanogr.* **51**: 12–20.
- Schoemann, V., S. Becquevort, J. Stefels, V. Rousseau, and C. Lancelot. 2005. *Phaeocystis* blooms in the global ocean and their controlling mechanisms: A review. *J. Sea Res.* **53**: 43–66.
- Seifert, M., B. Rost, S. Trimborn, and J. Hauck. 2020. Meta-analysis of multiple driver effects on marine phytoplankton highlights modulating role of pCO₂. *Glob. Chang. Biol.* **26**: 6787–6804.
- Sett, S., L. T. Bach, K. G. Schulz, S. Koch-Klavsen, M. Lebrato, and U. Riebesell. 2014. Temperature modulates coccolithophorid sensitivity of growth, photosynthesis and calcification to increasing seawater pCO₂. *PloS One* **9**: e88308.
- Smith, W. O., and S. Trimborn. 2023. *Phaeocystis*: A global enigma. *Ann. Rev. Mar. Sci.* **16**: 1–25.
- SoItwedel, T., and others. 2015. Natural variability or anthropogenically-induced variation? Insights from 15 years of multidisciplinary observations at the arctic marine LTER site HAUSGARTEN. *Ecol. Indicators*: 89–102.
- Søreide, J. E., E. Leu, J. Berge, M. Graeve, and S. Falk-Petersen. 2010. Timing of blooms, algal food quality and *Calanus glacialis* reproduction and growth in a changing Arctic. *Glob. Chang. Biol.* **16**: 3154–3163.
- Steinacher, M., and others. 2010. Projected 21st century decrease in marine productivity: A multi-model analysis. *Biogeosciences* **7**: 979–1005.
- Stoll, M. H. C., K. Bakker, G. H. Nobbe, and R. R. Haese. 2001. Continuous-flow analysis of dissolved inorganic carbon content in seawater. *Anal. Chem.* **73**: 4111–4116.
- Thoisen, C., K. Riisgaard, N. Lundholm, T. G. Nielsen, and P. J. Hansen. 2015. Effect of acidification on an Arctic phytoplankton community from Disko Bay, West Greenland. *Mar. Ecol. Prog. Ser.* **520**: 21–34.
- Thompson, P. A., M.-X. Guo, and P. J. Harrison. 1992. Effects of variation in temperature. I. On the biochemical composition of eight species of marine phytoplankton. *J. Phycol.* **28**: 481–488.
- Tilzer, M. M., M. Elbrächter, W. W. Gieskes, and B. Beese. 1986. Light-temperature interactions in the control of photosynthesis in Antarctic phytoplankton. *Polar Biol.* **5**: 105–111.
- Toseland, A., and others. 2013. The impact of temperature on marine phytoplankton resource allocation and metabolism. *Nat. Clim. Change* **3**: 979–984.
- Verity, P. G., T. J. Smayda, and E. Sakshaug. 1991. Photosynthesis, excretion, and growth rates of *Phaeocystis colonies* and solitary cells. *Polar Res.* **10**: 117–128.
- Verity, P. G., C. P. Brussaard, J. C. Nejtgaard, M. A. van Leeuwe, C. Lancelot, and L. K. Medlin. 2007. Current understanding of *Phaeocystis* ecology and biogeochemistry, and perspectives for future research. *Biogeochemistry* **83**: 311–330.
- Vernet, M., T. L. Richardson, K. Metfies, E.-M. Nöthig, and I. Peeken. 2017. Models of plankton community changes during a warm water anomaly in arctic waters show altered trophic pathways with minimal changes in carbon export. *Front. Mar. Sci.* **4**: 4.
- White, E., C. J. M. Hoppe, and B. Rost. 2020. The Arctic picoeukaryote *Micromonas pusilla* benefits from ocean acidification under constant and dynamic light. *Biogeosciences* **17**: 635–647.
- Wolf, K. K. E., C. J. M. Hoppe, and B. Rost. 2018. Resilience by diversity: Large intraspecific differences in climate change responses of an Arctic diatom. *Limnol. Oceanogr.* **63**: 397–411.
- Wollenburg, J. E., and others. 2018. Ballasting by cryogenic gypsum enhances carbon export in a *Phaeocystis* under-ice bloom. *Sci. Rep.* **8**: 7703.
- Young, J. N., J. A. L. Goldman, S. A. Kranz, P. D. Tortell, and F. M. M. Morel. 2015. Slow carboxylation of Rubisco constrains the rate of carbon fixation during Antarctic phytoplankton blooms. *New Phytol.* **205**: 172–181.
- Zhang, Y., M. Yamamoto-Kawai, and W. J. Williams. 2020. Two decades of ocean acidification in the surface waters of

the Beaufort gyre, Arctic Ocean: Effects of sea ice melt and retreat from 1997–2016. *Geophys. Res. Lett.* **47**: e60119.

Acknowledgments

We acknowledge the help of Claudia Burau and Prof. Dr. Boris Koch in the measurements and quality controls of DOC/N samples and thank an anonymous reviewer for valuable comments. Open Access funding enabled and organized by Projekt DEAL.

Conflict of Interest

None declared.

P. pouchetii under multiple drivers

Submitted 17 April 2023

Revised 29 August 2023

Accepted 07 November 2023

Associate editor: David Antoine